

## Transport Channel Regulated MXene Membrane *via* Organic Phosphonic Acids for Efficient Water Permeation

Ming Yi <sup>a,b,c</sup>, Frédéric Héraly <sup>c</sup>, Jian Chang <sup>c</sup>, Atefeh Khorsand Kheirabad <sup>c</sup>, Jiayin Yuan <sup>c</sup>,  
Yan Wang<sup>\*a,b</sup> and Miao Zhang<sup>\*c</sup>

<sup>a</sup> Key Laboratory of Material Chemistry for Energy Conversion and Storage (Huazhong University of Science and Technology), Ministry of Education, Wuhan, 430074, P. R. China

<sup>b</sup> Hubei Key Laboratory of Material Chemistry and Service Failure, School of Chemistry and Chemical Engineering, Huazhong University of Science & Technology, Wuhan, 430074, P. R. China

<sup>c</sup> Department of Materials and Environmental Chemistry, Stockholm University, Stockholm, 10691, Sweden

\* Corresponding author.

E-mail address: wangyan@hust.edu.cn (Yan Wang)

E-mail address: miao.zhang@mmk.su.se (Miao Zhang)

## Experimental section

### **Materials**

All chemicals from chemical suppliers were used as received without any further purification. High purity ( $\geq 99\%$ )  $\text{Ti}_3\text{AlC}_2$  MAX phase powder (400 mesh) was purchased from Laizhou Kai Kai Ceramics Materials Co., Ltd. Hydrochloric acid (HCl, 37 %) was supplied from VWR International. Dopamine hydrochloride, Tris (hydroxymethyl) aminomethane (THAM,  $\geq 99.8\%$ ), Copper sulfate ( $\text{CuSO}_4$ ,  $\geq 99.99\%$ ), Lithium fluoride (LiF,  $\geq 99.98\%$  trace metals basis), Iminodi(methylphosphonic acid) (**2P**, 97%), Nitrilotri(methylphosphonic acid) (**3P**,  $\geq 97\%$ ), phytic acid solution (**PA**, 50%), Diethylenetriaminepentakis(methylphosphonic acid) solution (**5P**, 50%), Congo Red (CR,  $\geq 35\%$ ), Eriochrome black T (BT, indicator grade), Methylene blue (MB,  $\geq 97.0\%$ ), Rose Bengal (RB, 95%) were ordered from Sigma-Aldrich. Nylon-66 commercial microfiltration membrane was purchased from Tianjing JinTeng Experiment Equipment Co., Ltd. Deionized (DI) water was used throughout the experiment unless particularly stated.

### **Synthesis of Mxene:**

MXene dispersion was synthesized following the minimally intensive layer delamination (MILD) method as reported previously,<sup>1</sup> with minor modification. In detail, 1.5 g high purity MAX powder (equivalent of 12 M) was cautiously added into the mixture of 30 mL 9 M HCl and 2.4 g LiF under continuously stirring over the course of 10 min (ice bath). The etching reaction was

stirred and kept for 36 h at room temperature. Then the multilayer  $\text{Ti}_3\text{AlC}_2$  and unetched MAX particles were washed and centrifuged (10000 rpm and one hour for each cycle) with DI water until the supernatant reached a pH value about 6.  $\text{Ti}_3\text{C}_2\text{T}_x$  sheets suspension was produced by the exfoliation process of resultant slurry under ultrasonication for 1 h under the  $\text{N}_2$  flow environment. The concentration of  $\text{Ti}_3\text{C}_2\text{T}_x$  suspension was obtained by calculating the weight of dry  $\text{Ti}_3\text{C}_2\text{T}_x$  sheets.

### **PDA coating of nylon-66 substrate:**

Dopamine hydrochloride (2 mg/mL) was dissolved in an aqueous solution (pH = 8.5, mM) containing tris (hydroxymethyl) aminomethane (THAM) and  $\text{CuSO}_4$  (5 mM). A nylon-66 substrate was immersed in the dopamine THAM buffer solution for 3 h at 40 °C. Subsequently, it was washed by DI water to remove the residual PDA solution and then stored in DI water prior to use.

### **Fabrication of OPA modified Mxene membrane:**

A certain amount of  $\text{Ti}_3\text{C}_2\text{T}_x$  suspension was added into OPA solution dropwise with stirring for a certain time at room temperature. PA solution with the concentration varied from 0 – 4.0

wt% was applied for the concentration optimization of the modifier. The concentration of 2P, 3P and 5P solution was controlled as the equal molar ratio of PA solution. After the modification of OPA molecules, the resultant  $Ti_3C_2T_x$  suspensions were vacuum filtrated on PDA-coated nylon-66 supports to obtain the MXene membranes. [S1].

### **Characterizations:**

The morphology of the membrane was characterized by scanning electron microscopy (SEM, JEOL 7000, Japan) operated at 5 kV, and the element distribution was detected with the energy dispersive X-ray spectroscopy (EDX) of SEM. The transmission electron microscopy (TEM, JEOL JEM-2100F, Japan) and selected area electron diffraction (SAED) studies were performed under an accelerating voltage of 100 kV. Atomic force microscopy (AFM, Veeco Instruments, CA) was conducted utilizing a Nanoscope V in tapping mode. Powder X-ray diffraction (PXRD, Bruker, D8 Advance, America) patterns of the membrane were collected using *Cu-K $\alpha$*  radiation at 40 kV and 40 mA in the  $2\theta$  angle range of  $5^\circ$  to  $90^\circ$ , with the scan step of  $0.02^\circ$ . Zeta potential and dynamic light scattering (DLS) measurements were performed on a Zetasizer (Malvern, England). X-ray photoelectron spectroscopy (XPS, Thermo Fisher, Escalab 250XI, America) analysis was carried out using a monochromatic *Al-K $\alpha$*  X-ray source ( $h\nu = 1486.6$  eV) operated at 150 W. Water contact angle (WCA) of the membrane surface was measured with a Geniometer (Krüss, DSA25, Germany) at ambient conditions.

### **Nanofiltration (NF) performance tests of MXene membrane**

The separation performance of the membrane was evaluated using a lab-scale cross-flow NF filtration set up (Suzhou Faith & Hope Membrane Technology Co. Ltd.) with an effective area of  $10.75$  cm<sup>2</sup>. Before testing, the membrane was pre-filtrated with DI water at 2 bar until the flux reached a steady state. The permeance was then collected under the operational pressure of 1 bar with the crossflow rate of 40 L/h. Various dye solutions (BT, CR, MB, RB) with the concentration of 100 ppm were employed as the feed solution for the tests. The permeability of the membrane was calculated using the following equation:

$$Permeability = \frac{V}{A \times t \times P} \quad (1)$$

where  $V$  is the permeate volume (L);  $A$  is the effective membrane area ( $m^2$ );  $t$  is the filtration time (h).  $P$  is the operating pressure, fixed at 1 bar.

The dye rejection (R) was calculated as the following equation:

$$Rejection = \left(1 - \frac{C_p}{C_f}\right) \times 100 \quad (2)$$

where  $C_f$  and  $C_p$  are the dye concentrations in the feed and permeate, respectively. The concentration was measured by a UV-Vis spectrophotometer (Thermo Fisher, GENESYS 150, America).

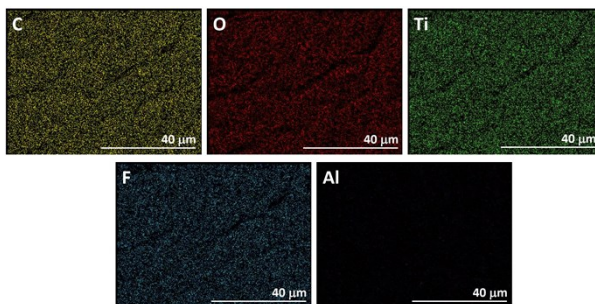


Fig. S1. EDS mapping of pure Ti<sub>3</sub>C<sub>2</sub>T<sub>x</sub> nanosheets membrane.

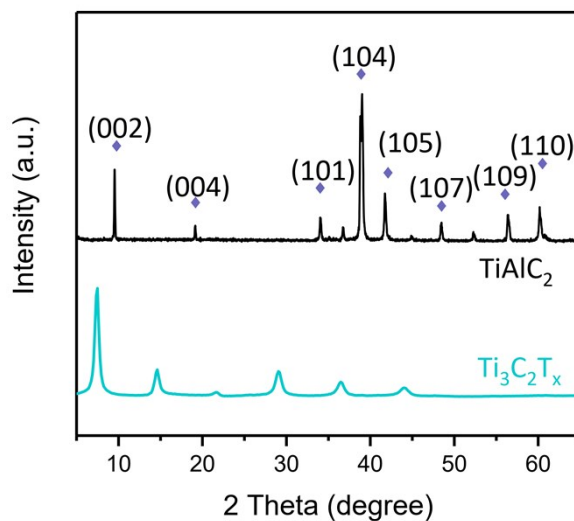


Fig. S2. XRD patterns of bulk Ti<sub>3</sub>AlC<sub>2</sub> and Ti<sub>3</sub>C<sub>2</sub>T<sub>x</sub> nanosheets.

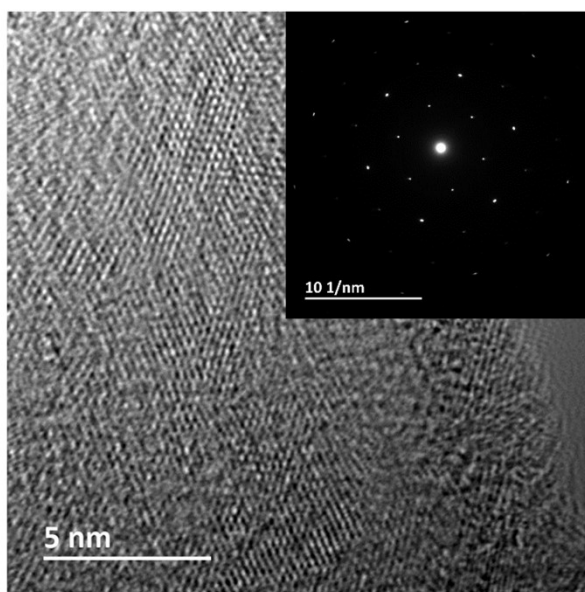


Fig. S3. HRTEM image (inset shows the SAED patterns) of  $Ti_3C_2T_x$  nanosheets.

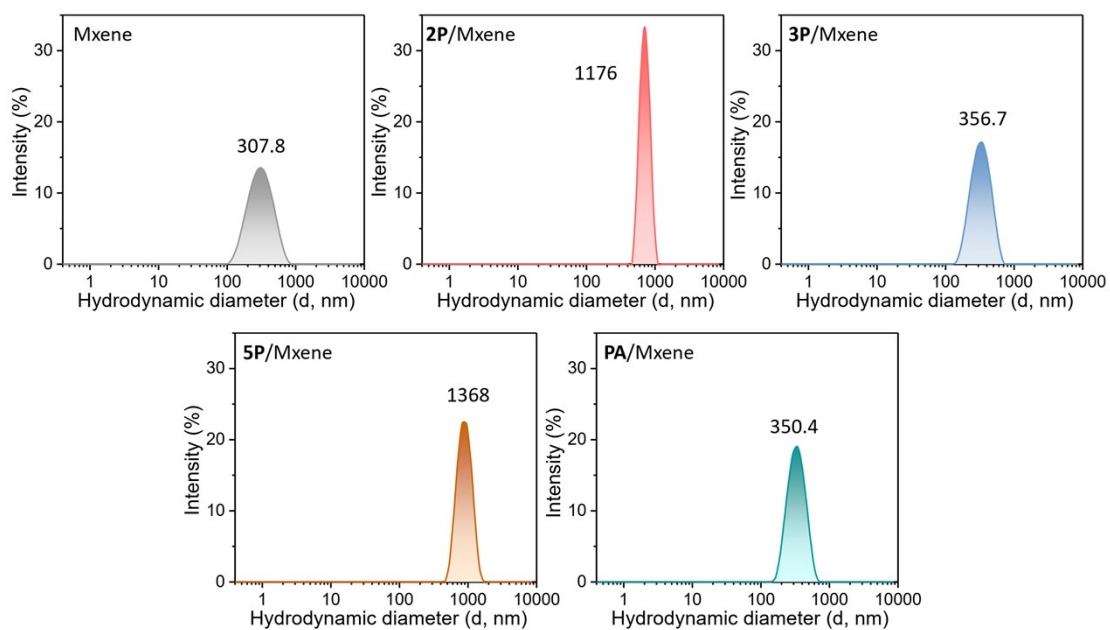


Fig. S4. DLS results of pure and OPA modified  $Ti_3C_2T_x$  nanosheets suspensions.

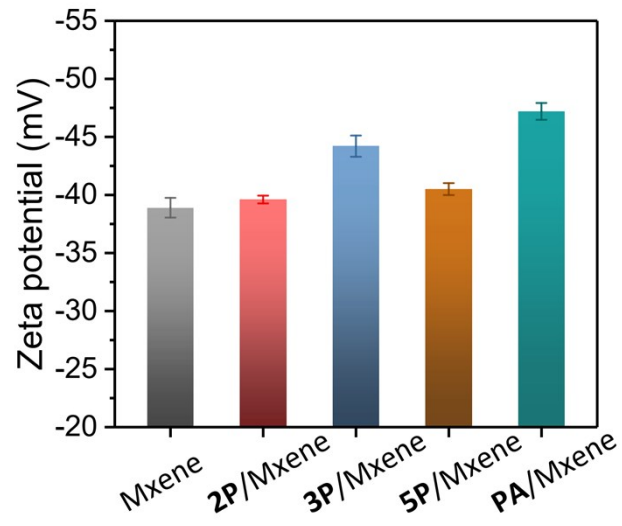


Fig. S5. Zeta potentials of pure and OPA modified  $Ti_3C_2T_x$  nanosheets suspensions.



Fig. S6. The digital photos of pure and OPA modified  $Ti_3C_2T_x$  nanosheets suspensions after 12-h reaction.

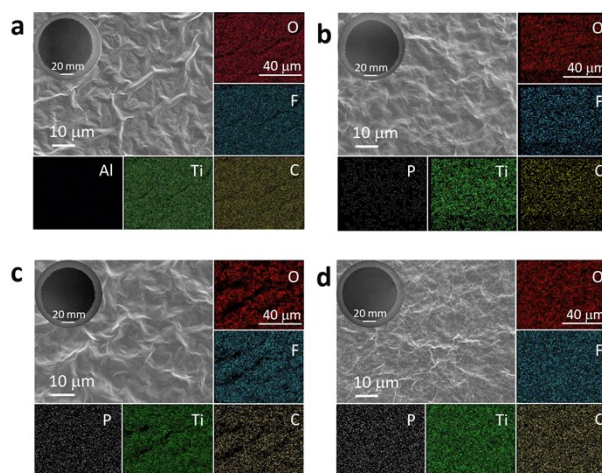


Fig. S7. SEM images and mapping of (a) pure, (b) **2P**/MXene, (c) **3P**/MXene, and (d) **5P**/MXene membrane. Inset shows the digital photo of the corresponding membrane on nylon-66 support.

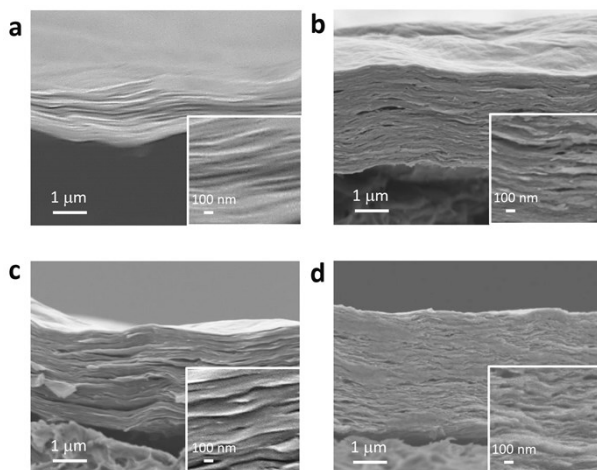


Fig. S8. Cross-sectional SEM images of (a) pure, (b) **2P**/MXene, (c) **3P**/MXene, and (d) **5P**/MXene membranes.

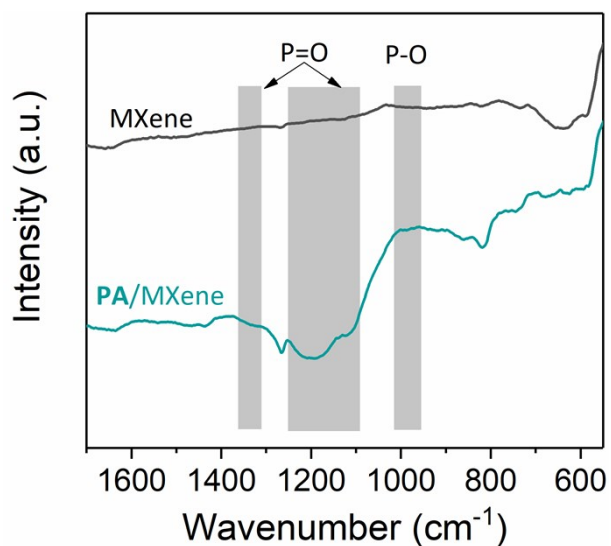


Figure S9. FT-IR spectra of pure and **PA**/MXene power.

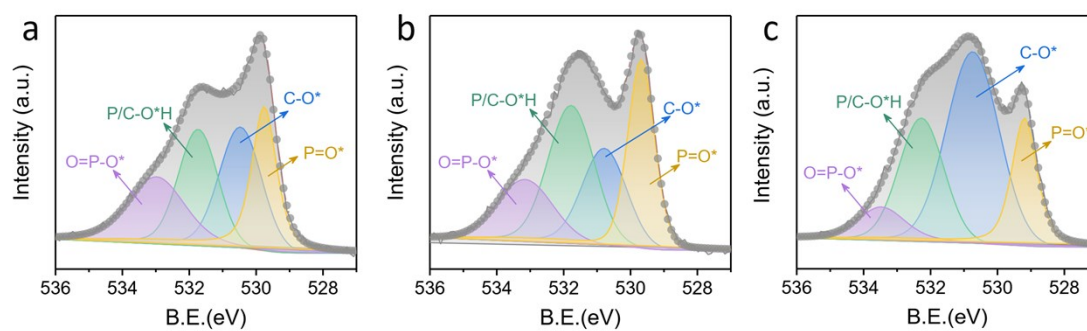


Fig. S10. Peak deconvolution of narrow-scan spectra of O 1s for (a) **2P**/MXene, (b) **3P**/MXene, and (c) **5P**/MXene membranes.

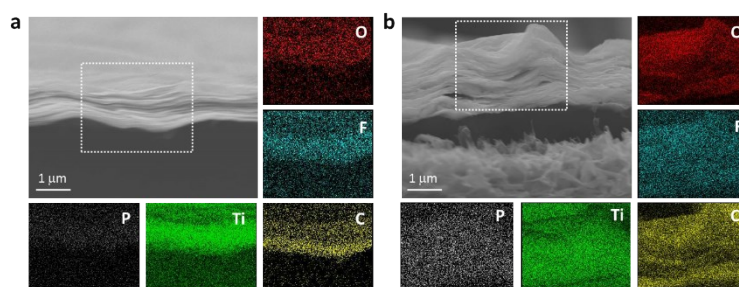


Fig. S11. The cross-sectional EDS mapping of (a) pure and (b) OPA modified MXene membranes.



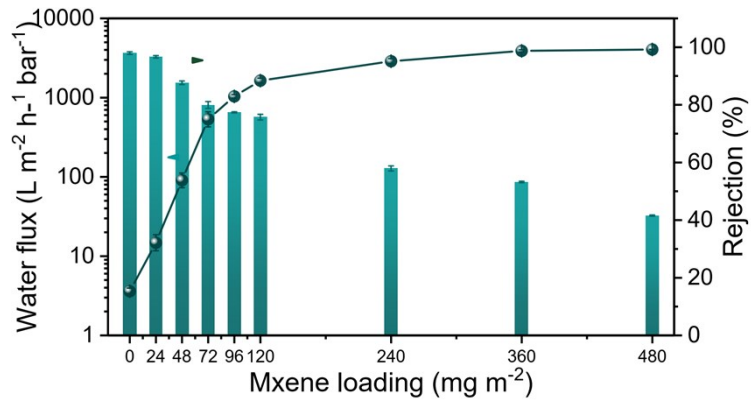


Fig. S12. The effect of MXene loading on the separation performance of the MXene membrane.

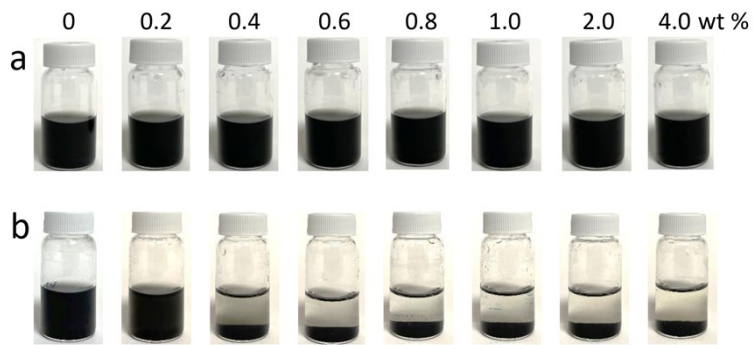


Fig. 13. The digital photos of  $Ti_3C_2T_x$  nanosheets suspensions mixed with different amount of PA. (a) Just mixed, (b) after 12-h reaction.

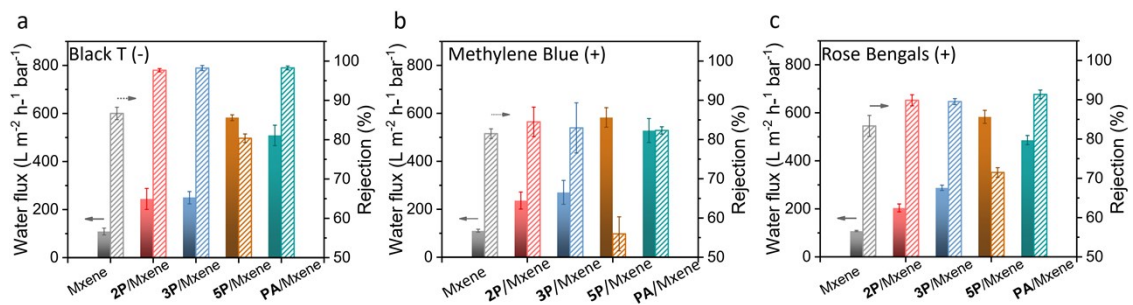


Fig. S14. Separation performance of pure and OPA modified MXene membrane for (a) BT, (b) MB and (c) RB. (Feed concentration: 100 ppm, operational pressure: 1 bar, crossflow rate: 40 L/h)

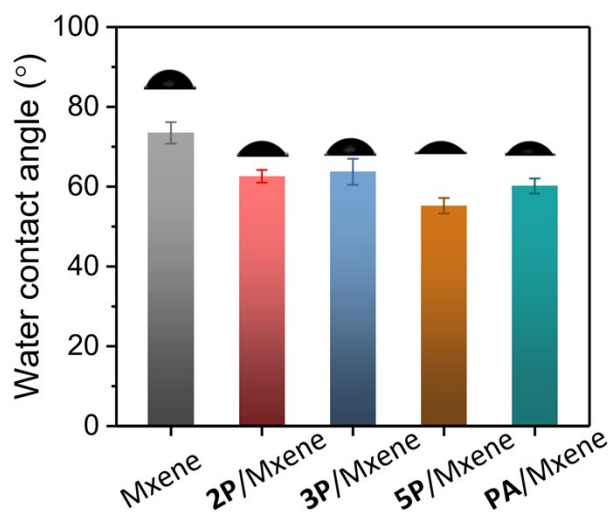


Fig. S15. Water contact angles of the pure and OPA modified MXene membranes.

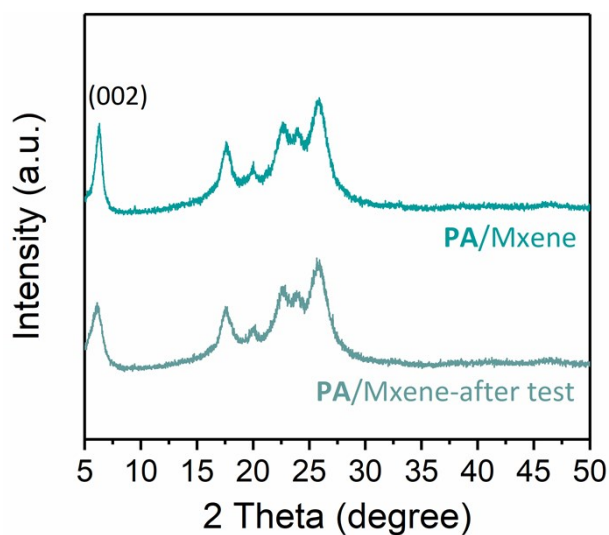


Fig. S16. XRD patterns of pure and PA/MXene membranes before and after 10-cycle of testing.

Table S1. Surface elemental composition of the pure and OPA modified MXene membranes by XPS analysis.

Membrane	Atomic percentage (%)				
	C 1s	O s	F 1s	Ti 2p	P 2p
Mxene	45.37	17.24	12.16	25.22	/
2P/Mxene	41.59	22.62	9.88	24.16	1.76

<b>3P/Mxene</b>	42.75	20.33	10.4	23.58	2.93
<b>5P/Mxene</b>	47.96	22.95	7.88	17.14	4.07
<b>PA/Mxene</b>	45.35	23.5	8.63	21.75	0.76

Table S2. Surface elemental composition of the pure and OPA modified MXene membranes by EDS analysis.

Membrane	Atomic percentage (%)				
	C K	O K	F K	Ti K	P K
Mxene	41.74	32.33	25.92	0.01	/
<b>2P/Mxene</b>	37.41	39.28	20.95	0	1.93
<b>3P/Mxene</b>	41.05	35.54	17.6	0	5.81
<b>5P/Mxene</b>	49.64	29.14	15.27	0	5.96
<b>PA/Mxene</b>	37.63	42.17	18.08	0	2.11

Note: The signal of Ti element was overlapped with that of O, thus zero atomic percentage of Ti.

Table S3. Benchmarking of MXene membranes for dyes nanofiltration.

Membrane type	Operational pressure (bar)	Permeance (L/m <sup>2</sup> h bar)	Dye rejection (%)	Molecular weight (g/mol)	Feed conc. (mg/L)	Ref.
RGO/PDA/MXene	1	174.2	95	319.9	20	<sup>2</sup>
Mxene	2	28.94	94.7	319.9	75	<sup>3</sup>
Mxene	1	340.5	95.1	514.4	100	<sup>4</sup>
Crumpled Mxene	5	357	67.7	960.8	20	<sup>5</sup>
GO/Mxene	5	16.7	98.6	319.9	10	<sup>6</sup>
Mxene-230	1	2302	96.3	1111.1	/	<sup>7</sup>
Mxene	1	1084	90	960.8	/	<sup>8</sup>
<b>PA/Mxene</b>	1	514.5	99.6	696.7	100	This work
<b>PA/Mxene</b>	1	508.6	98.3	416.4	100	This work

## References

1. H. Chen, Y. Wen, Y. Qi, Q. Zhao, L. Qu and C. Li, *Adv. Funct. Mater.*, 2019, **30**, 1906996.
2. X. F. Feng, Z. X. Yu, R. X. Long, Y. X. Sun, M. Wang, X. H. Li and G. Y. Zeng, *Sep. Purif. Technol.*, 2020, **247**, 116945.
3. S. Y. Zhang, S. Y. Liao, F. Y. Qi, R. T. Liu, T. H. Xiao, J. Q. Hu, K. X. Li, R. B. Wang and Y. G. Min, *J. Hazard. Mater.*, 2020, **384**, 121367.
4. Z. K. Li, Y. Wei, X. Gao, L. Ding, Z. Lu, J. Deng, X. Yang, J. Caro and H. Wang, *Angew. Chem.*, 2020, **59**, 9751-9756.
5. Y. D. Xing, G. Akonkwa, Z. Liu, H. Q. Ye and K. Han, *ACS Appl. Nano Mater.*, 2020, **3**, 1526-1534.
6. S. C. Wei, Y. Xie, Y. D. Xing, L. C. Wang, H. Q. Ye, X. Xiong, S. Wang and K. Han, *J. Membr. Sci.*, 2019, **582**, 414-422.
7. J. Wang, P. Chen, B. Shi, W. Guo, M. Jaroniec and S. Z. Qiao, *Angew. Chem.*, 2018, **57**, 6814-6818.
8. L. Ding, Y. Y. Wei, Y. J. Wang, H. B. Chen, J. Caro and H. H. Wang, *Angew. Chem.*, 2017, **56**, 1825-1829.